Visual Abstract

Improvement of mechanical properties of railway track concrete sleepers using ultra high performance concrete (UHPC)

Sayed Ahmed, Hossam Atef, Mohamed Husain
Zagazig University, Egypt
sayedahmed.str@gmail.com, eng_hossam.atif@outlook.com, Mo_husain2000@yahoo.com

ABSTRACT. In recent times, the shape of the beams evolved from wooden sleepers and then to steel sleepers until they reached concrete sleepers. These sleepers play a significant role in transferring the loads from the train wheels to the subgrade layers fixed by the railway. This development took place in concrete sleepers until we reached mono-block concrete sleepers. This paper discusses, through laboratory experiments, the effect of ultra-high performance concrete mixtures on the behavior of mono-block concrete sleeper B70. The ability of these new sleepers to resist train loads was also studied compared to its conventional concrete sleepers. This research aimed to determine through experiment if these sleepers' behavior fulfilled the European requirements standers for prestressed concrete sleepers and make comparisons between the UHPC sleepers and conventional concrete sleepers. These sleepers were tested under static load tests at the rail seat and center section and pull-out tests for cast-in fastening components. These initial results suggest that a new generation of Ultra-high performance concrete sleepers can be created; the long-term efficiency of this category of sleeper will need to be confirmed by dynamic and fatigue tests and practical use.

KEYWORDS. Railway sleeper; Ultra high performance concrete (UHPC).

OPEN ACCESS

Citation: Ahmed, S., Atef, H., Husain, M., Improvement of mechanical properties of railway track concrete sleepers using ultra high performance concrete (UHPC), 60 (2022) 243-264.

Received: 01.12.2021
Accepted: 05.02.2022
Online first: 08.02.2022
Published: 01.04.2022

INTRODUCTION

Transportation is an essential means in developing societies. And one of the most important of this transportation is the railway network. It is considered the most effective means of transporting passengers and goods. These days, the railway connects cities in the same country. It also links countries and intertwines networks of a state with those of its neighbors, and often we find an entire continent linked by a great network of railways. This research focuses on the ballasted railway tracks, which have extensively been constructed in Egypt. Railway components can be divided into two main parts: substructure and superstructure. Subgrade and ballast are components of substructure; in addition, rails, rail

pads, fastening systems, and railway concrete sleepers are components of the superstructure [1,2]. Fig.1 shows the main components of a rail track system.

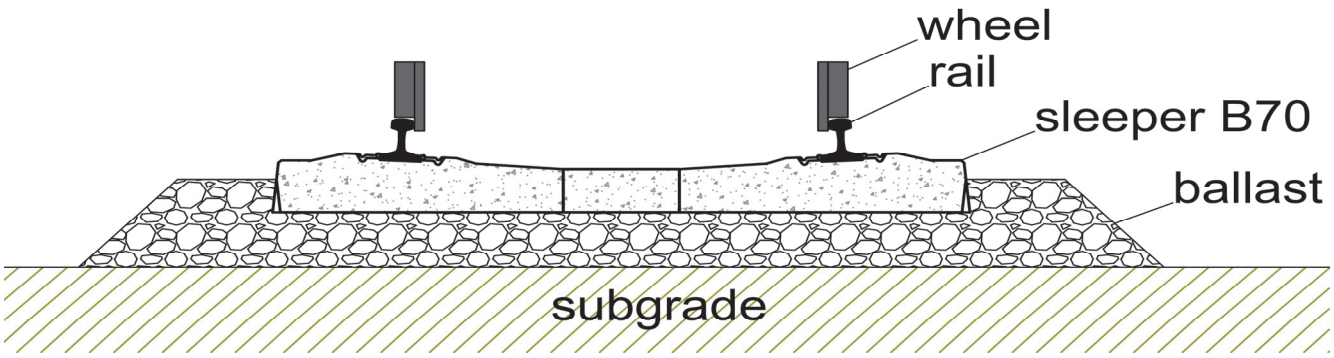

Figure 1: Components of ballast track.

The sleepers play an essential role in stabilizing railway components. It resists the lateral and longitudinal loads caused by moving rolling stock over the railway [3]. There are three main types of sleepers; timber sleeper, steel sleeper, and concrete sleeper. The most common sleeper material was hardwood timber, which was also the first to use in railway networks. At this time, the average number of timber sleepers used in the railways could reach up to 2.5 billion for worldwide [4]. On the other hand, it has many Disadvantages like; Exposure to wear and tear, which leads to a shortening of its useful life, easily exposed to fire hazards, and difficulty to preserve the gauge [5]. In addition, the use of steel sleepers is limited for the following reasons; increasing the steel cost, being liable to corrode, the difficulty of maintenance, and sensitivity to chemical attacks [5,6].

Recently, concrete sleepers are becoming more popular in the railway field, especially prestressed concrete sleepers [3]. However, they have gradually replaced timber and steel sleepers [7]. On the other hand, concrete sleepers have a longer lifespan than their wooden sleepers counterparts, reaching 50 years [8]. Concrete sleepers are an excellent choice for a variety of reasons. The heavyweight for the concrete sleeper adds to the track's strength and stability. They keep track in better gauge, cross-level, and alignment. They are poor conductors of electricity, and in most cases, they can be produced by using locally available resources [5]. Now, most studies focus on improving the design of concrete mixes to improve the behavior of concrete sleepers and to rise their design life [9,10].

Over time, the forms of concrete mixture developed to obtain concrete with high compressive and flexure strength until studies reached ultra high performance concrete. UHPC typically contains cement, silica fume, fine sand, high-range water-reducing admixtures, and water binder ratios (w/b), generally ranging between 0.15 and 0.25 [11]. Ultra high performance concrete (UHPC) represents the main step forward when compared to traditional normal strength concrete (NSC) and high strength concrete (HSC) due to the achievement of very high strength and very low permeability [12]. Moreover, UHPC is promising in significantly improving deteriorating concrete structures' structural strength and durability. This is due to the material's resistance to environmental degradation and high mechanical loading [13]. The main principles of UHPC mix are (i) improvement homogeneity; (ii) improvement compaction; (iii) improvement of the microstructure by heat treatment; (iv) improvement ductility; (v) mixing and casting procedures as close as possible to existing practice [14]. Because of the high cost of producing UHPC, part of the cement quantity can be replaced by some industrial by-products such as ground granulated blast-furnace (GGBS) and silica fume (SF). Yu [15] developed the UHPFRC with different mixtures by different amounts of cement, GGBS, and silica fume. Tayeh [16] used UHPFRC as a repair material using 768 kg/m^3 cement and 192 kg/m^3 silica fume. Generally, UHPC has a unique combination of high strength, ductility, and durability properties compared to all the other types of concrete [17].

Despite successful UHPC research and applications in the concrete construction sector, current guidelines have yet to provide a standard norm. The recommendations are still in their early stages due to limited literature in the railway field. The present study investigates the manufacture of B70 sleepers with ultra high performance concrete and comparison with the traditional concrete mix for the same sleepers. This study is based on the common approach of sleeper manufacture in Egypt. Three tests were carried out on B70 sleepers under optimized laboratory conditions, the positive bending moment under the rail seat, the negative bending moment at the middle span of sleeper, and the pull-out test following the European standard to verify the suitability of these new sleepers [18,19].

TECHNICAL SPECIFICATIONS OF B70 CONCRETE SLEEPERS

The mono-block sleepers (B70) with Vossloh W14 rail fastening and rail type UIC 54 are used in this research. These sleepers have the length and gauge 2400 mm and 1435 mm, respectively. However, they have a cant of 1 in 20 at the rail seat section surface to set the rail UIC 54. In addition, they are prestressed with four wires, which diameter and length are (9.4 – 2337) mm, respectively, according to the European standard [20]. Moreover, the approximate weight is 260 kg, and the Supporting Surface Area is 6220 cm². The Geometrical dimensions of the mono-block sleeper B70 are presented in Tab. 1. Moreover, a schematic of the shape of a concrete B70 sleeper is given in Fig. 2.

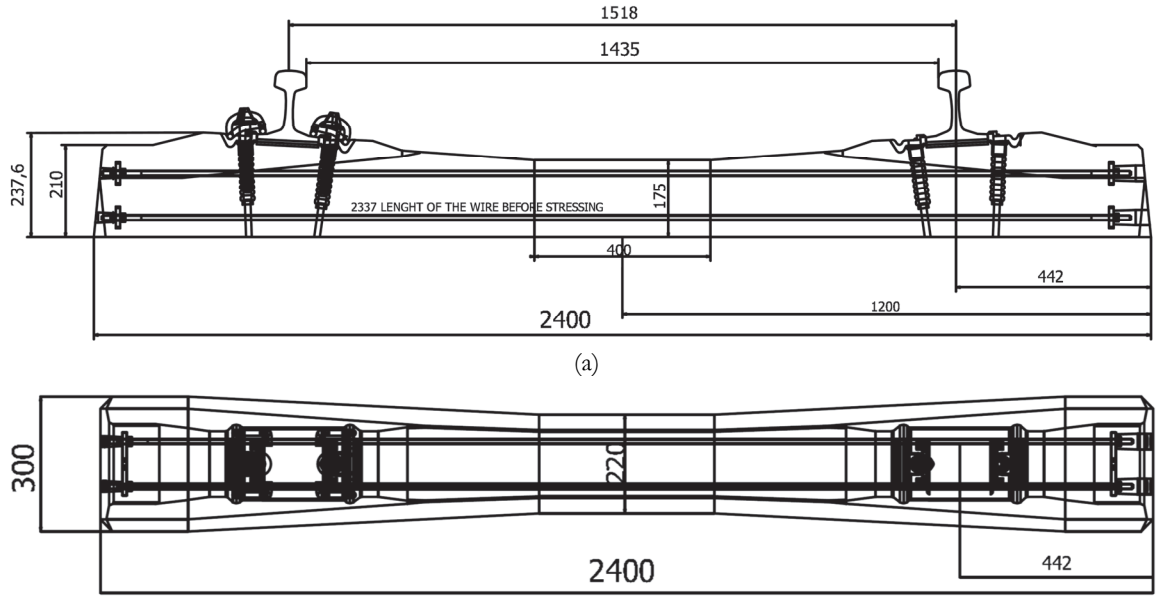

Figure 2: Geometrical dimension of mono-block sleeper B70 (unit: mm): (a) front view; (b) top view.

Sleeper geometry	B70 sleeper
Length	2400mm
Width at the sleeper end	300mm
Width under rail seat axis	275mm
Depth under rail seat	214mm
Width in center	220mm
Depth in center	175mm
Rail seat cant	1 in 20
Rail seat center spacing	1518mm
Weight	250-260kg

Table 1: Technical specifications of B70 concrete sleepers.

FABRICATION OF SLEEPERS

Traditional concrete mix of sleepers

Siegwart factory in Egypt produces mono-block concrete sleepers (B70) with conventional concrete. Mono-block concrete B70 contains ordinary Portland cement with high grade (42.5R) 400 kg/m^3. Moreover, it has contained yellow 509 kg/m^3 sand with a maximum particle size of 5mm. In addition, it has three sizes of dolomite; size 5/11 = 312 kg/m^3, size 11/22 = 309 kg/m^3, and size 22/30 = 315 kg/m^3. It contains water from 100 to 120 L/m^3. Compressive strength for standard cube 15 cm is for 7 days minimum 35 MPa and for 28 days minimum 50 MPa. Tab. 2 shows the material properties. Fig. 3 shows the material for this mix.

Materials	Type	Specific density (kg/m^3)
Cement	CEM I 42.5 N	3280
	CEM I 52.5 N	3150
Fine sand	Micro sand	2720
Coarse sand	Sand 0-2	2640
	Sand 0-5	2530
Silica fume	Micro silica	2200
superplasticiser	Polycarboxylate ether	1050

Table 2: Data of material.

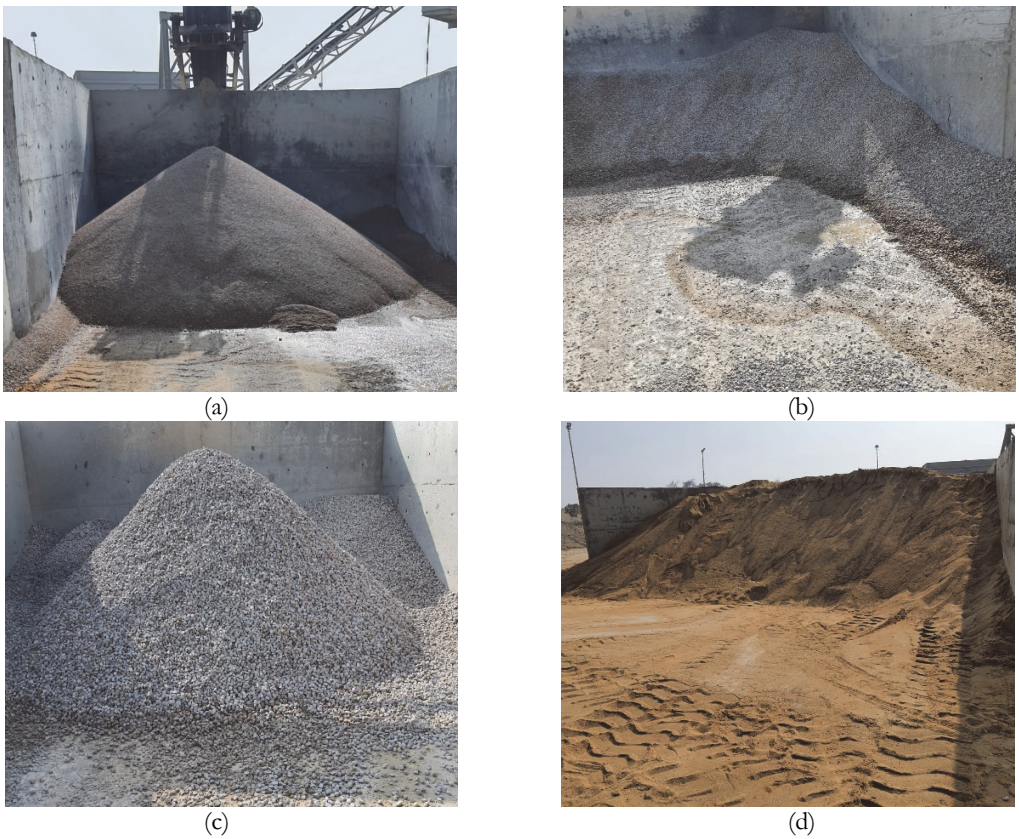

(a) (b) (c) (d)

Figure 3: Material for traditional mix. (a) dolomite 0/5; (b) dolomite 5/11; (c) dolomite 11/22; (d) yellow sand.

Mix design of UHPC specimens

In this research, the mix design of ultra high performance concrete depends on the mix of Yu [21], which presented the mix design based on the particle packing theory (Andreasen and Andersen (A&A) model and the modified A&A model). This mixture is the following, (i) Ordinary Portland cement with high grade 52.5N with 874.9kg/m^3; (ii) Micro sand with maximum particle size 1mm with 218.7kg/m^3; (iii) Friction sand with maximum particle size 2mm with 1054.7kg/m^3; (iv)

silica fume with 43.7kg/m³; (v) water with 202.1 kg/m³; (vi) superplasticiser with 45.9 kg/m³. Noted that Sika Fume-HR and Sikament 163M were used in this research instead of micro-silica and superplasticiser, respectively from Sika supplier in Egypt. In this research, the two mix designs used to cast conventional concrete and UHPC sleepers are shown in Tab. 3. Fig. 4 shows the material for the UHPC mix.

In this study, the mixing procedure to get UHPC mix follows the steps shown in [15,21]:

- Dry mixing is accomplished by placing all powders and sand fractions in the mixer for roughly 30s at low speed.
- After ensuring an overlap of all powder, put 75% of water in the mixer.
- Mixing for the 90s at low speed, then stopping the mixer for 30s.
- After that, put the remaining water and all amount of SP at low speed for 180s.
- Finally, make the mixer at high speed for 120s, then note that concrete converts from a dry case to a thick paste.

Materials	NC (kg/m³)	UHPC (kg/m³)
CEM I 52.5 N	-	874.9
CEM I 42.5 R	400	-
Dolomite 5/11	312	-
Dolomite 11/22	309	-
Dolomite 22/30	315	-
Micro sand	-	218.7
Sand 0-2	-	1054.7
Sand 0-5	509	-
Silica fume	43.7	43.7
Sikament 163M	45.9	45.9
Water	120	202.1

Table 3: Mix design.

Figure 4: Material for UHPC mix. (a) Cement; (b) Silica fume; (c) Sikament 163M; (d) Micro sand; (e) Yellow sand.

Production processes of sleepers

The mono-block sleepers are casting on the special steel mold shown in Fig. 5(a). Before casting, preparatory steps are taken to prepare the molds. First, the molds are lubricated. Second, the four wires are covered with plastic ducts. Third, these wires are attached to the anchor plate by dowels. Fourth, these wires are fixed to molds. Finally, the molds are ready for casting. The casting was done in layers and used the vibrator for the 30s to ensure full compaction for concrete. After the completion of the casting, the treatment is carried out through the steam room, as the traditional concrete sleepers are placed in those rooms for 8 hours under 550c temperature as following EN 13230-1 [22], while the UHPC sleepers were placed for 24 hours under the same temperature as following to Zongyun [23]. After steam curing, the sleepers demolded from molds and were air-cured for an additional 24h. Then, prestressing forces were applied with 250 kN for each wire. The compressive strength values at 7 days and 28 days for the two mixes of conventional concrete and UHPC are shown in Fig. 6. Tab. 4 shows the compressive strength at 28 days with different mixes from different references, which had the same components in this research in different proportions.

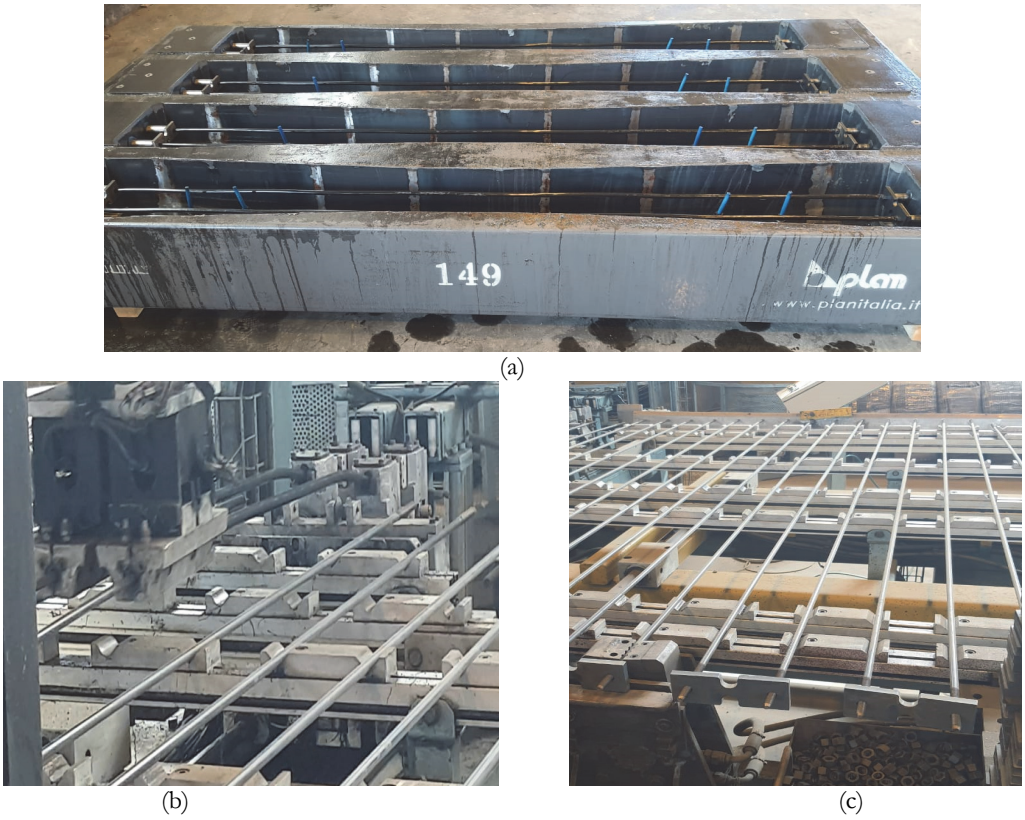

Figure 5: preparation method; (a) Lubrication the form; (b) covering wires; (c) anchor plate and nuts.

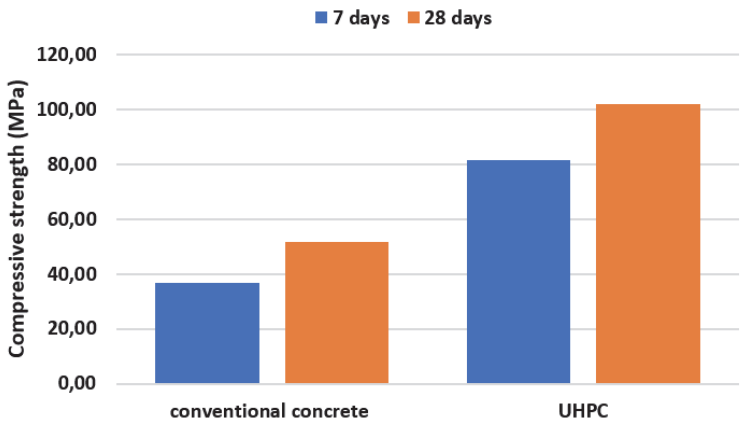

Figure 6: Compressive strength.

Reference	Cement (kg/m³)	Silica fume (kg/m³)	Limestone powder (kg/m³)	Water (kg/m³)	Compressive strength at 28 days (MPa)
Spiesz [15]	868.8	25	-	178.8	120
Qian [24]	400	200	500	200	105
Alani [25]	1080	-	-	184	138
Reddy [26]	800	200	-	200	120
Yu [27]	594.2	24.8	265.3	176.9	100

Table 4: Comparison of compressive strength.

TEST SETUP AND PROCEDURE

Requirement for performance tests

Several structural tests were carried out to verify the new structural design of UHPC sleepers following EN 13230-2 and EN 13481-2 [18,19]. Using Eqns. (1) and (2) to get Fr_0 and Fc_{on}, which are the reference tests loads at the rail seat section and the center section of the sleepers, respectively. Fr_0 was calculated by applying the design positive moment for the rail seat section (M_{dr+}). The design distance between the center of the rail seat section and the end edge of the sleepers, L_p is 0.441 m, which is in the range of $0.4 \leq L_p < 0.449$, so the L_r is 0.5 m as defined in EN 13230-2 [18]. While Fc_{on} was calculated by applying the design negative moment for the center section (M_{dc-}). In addition, the design distance between the centers of the rail seat section, L_c is 1.5 m.

$$Fr_0 = \frac{4M_{dr+}}{L_r - 0.1} = \frac{4 \times 13}{0.5 - 0.1} = 130KN \quad (1)$$

$$Fc_{0n} = \frac{4M_{dc-}}{L_c - 0.1} = \frac{4 \times 10}{1.5 - 0.1} = 28.6KN \quad (2)$$

Considering a 240 kN axle load, 140 Km/h of train speed, and a sleeper spacing of 0.6m according to the Egyptian National Railways (ENR), M_{dr+} and M_{dc-} were calculated to have values of 13 kN*m and 10 kN*m, respectively, according to UIC 713R and EN 13230-6 [28,29]. Moreover, the static coefficients (k_{1s} and k_{2s}) can be found in UIC 713R and EN 13230-6 [28,29]. Fr_r and Fc_{rn} are the loads when the initial crack begins at the rail seat section and the center section, respectively. $Fr_{0.05}$ and $Fr_{0.5}$ are the maximum loads' when a crack width becomes 0.05 mm and 0.5 mm at the rail seat section, respectively. Fr_B and Fc_{Bn} are the failure load at the rail seat section and the center section, respectively. P_0 is a tensile load that should not exceed 60 kN, and P_f is the maximum load at which the screw is removed from the sleeper according to EN 13481-2 [19]. All calculated structural requirements for each sleeper location are summarized in Tab. 5 to evaluate sleepers.

Test items	location	Requirements
Static bending test	Rail seat section	$Fr_r > Fr_0 = 130$ kN
		$Fr_{0.05} > k_{1s} \times Fr_0 = 1.8 \times 130 = 234$ kN
		$Fr_B > k_{2s} \times Fr_0 = 2.5 \times 130 = 325$ kN
	Center section	$Fc_n > Fc_{0n} = 30$ kN
		$Fc_B > k_{2s} \times Fc_{0n} = 2.5 \times 30 = 75$ kN
Pull out test	Rail seat	$P_f > P_0 = 60$ kN

Table 5: Performance criteria of sleepers.

Static bending test at rail-seat section

As known, the train load is directly applied through the rail and rail pad to the sleepers, so the rail-seat section should have adequate load resistance performance. For this purpose, three sleepers from each variable mix were carried out for the positive bending moment at the rail seat section according to EN 13230-2 [18]. A static bending test at the most critical section of these sleepers can investigate the impact of UHPC mix on traditional concrete sleepers. As shown in Fig. 7(a), the concrete sleeper's specimens were supported on plate supports and resilient pads with a center-to-center span length,

L_r, of 500 mm. The load was applied through the steel plate and rail pad, which was used to supply a uniform stress distribution at the top surface of the sleepers and to avoid local failure. A load cell with a capacity of 1000 kN was used to measure the applied load. Three linear variable differential transformers (LVDT) were installed on the sleepers. One of them was installed underneath the sleepers to measure the displacement at the rail seat section, and the other two LVDT were installed on the up and down of the sleeper to measure the width of the crack with an accuracy of up to 0.001 mm, as shown in Fig. 7(a). The load was applied according to EN 13230-2, and the loading protocol is shown in Fig. 7(b) as a present by Yang et al and Yoo et al [18,30,31]. The loading protocol was divided into 3 steps. First, increase the load with a load rate of 120 kN/min until reaching the Fr_0 load. Second, the load was increased by 10 kN for each step until it reached the first crack formation, Fr_r. Third, the load was increased by 20 kN for each step until it reached the ultimate failure load at the rail seat section, Fr_B. At steps 2 and 3, all the crack propagation and widths were measured by LVDT [30].

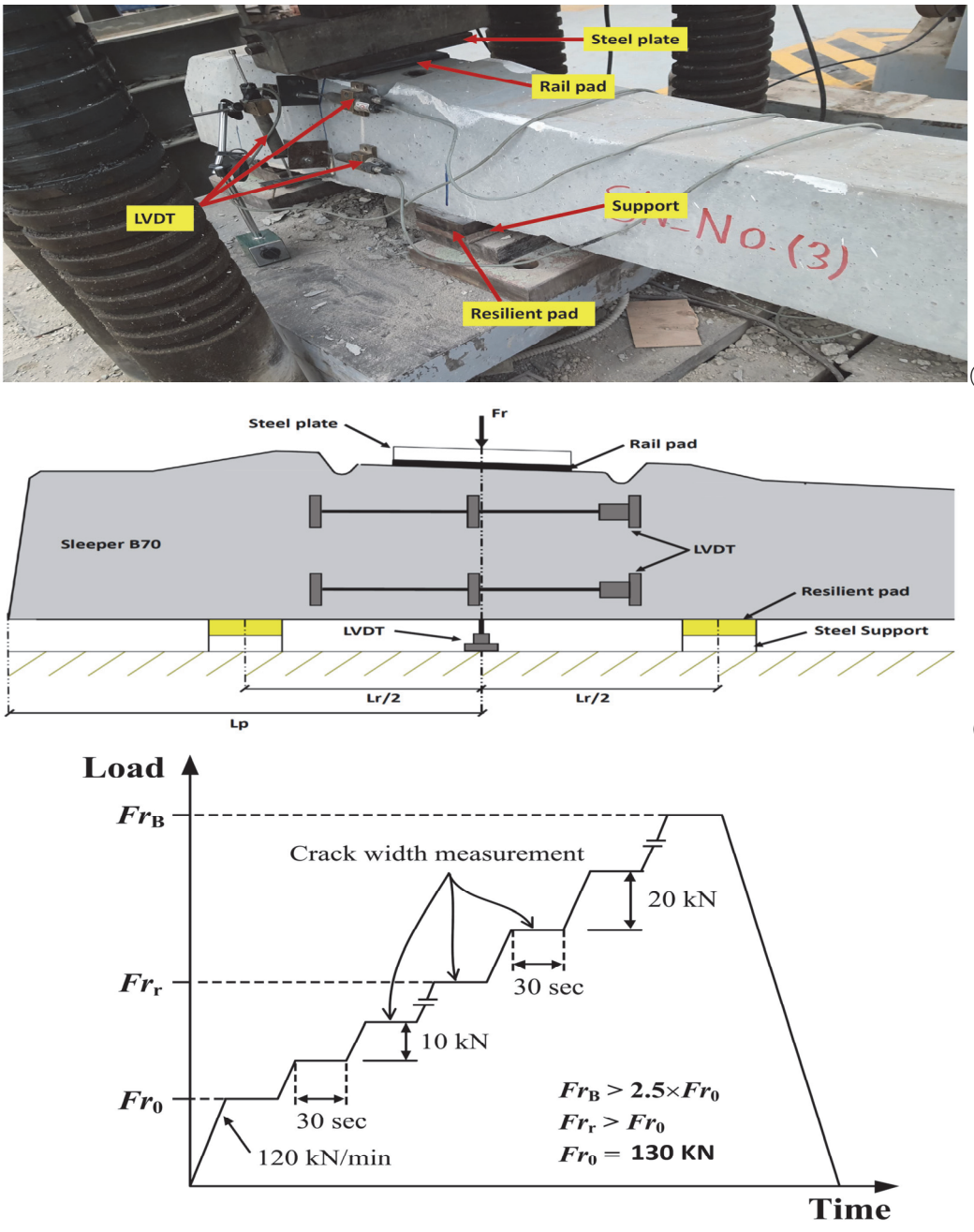

Figure 7: Static bending test at rail seat section: (a) test setup; (b) test setup sketch; (c) loading protocol [30,31].

Static bending test at center section

To investigate the static performance at the center section of the sleepers and to confirm the consistency of the fabrication of the UHPC sleepers, two sleepers from each variable mix were carried out for the negative bending moments at the center section according to EN 13230-2 [18]. As shown in Fig. 8(a), a sleeper was reversely seated on two supports and resilient pads with a center-to-center span length, L_c, of 1500 mm. From eq. (2), the negative initial reference test load for the center section, Fc_{0n}, was found as 28.6 kN. As in the previous test, three linear variable differential transformers (LVDT) were installed on the sleepers. One of them was installed in the middle under the sleeper to measure the mid-span deflection during the test, and the others were installed on the up and the down width of the sleeper in the middle span of the sleeper to measure the crack width, as shown in Fig. 8(a). The load was applied according to EN 13230-2, and the loading protocol is shown in Fig. 8(b) [18]. The loading protocol was divided into 2 steps. First, the loading was applied up to Fc_{0n} with a 120 kN/min loading rate. Second, the load was increased by 5 kN for each step until it reached the first crack formation, Fc_{rn}, and continued increasing until the center section no longer supported it, Fr_B.

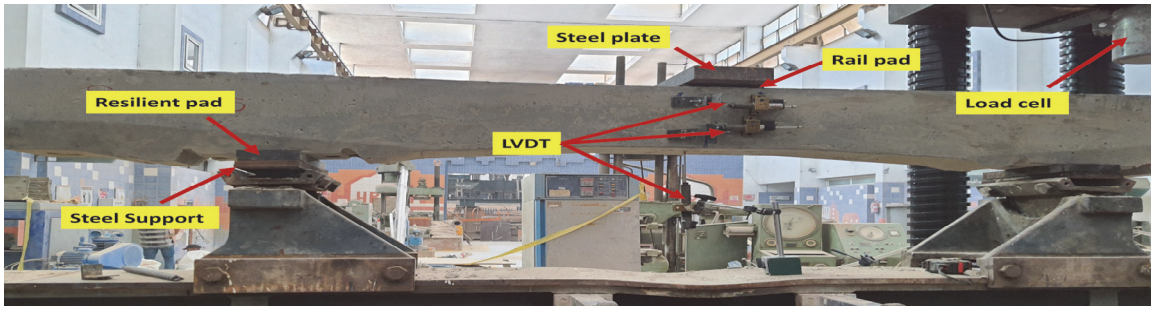

(a)

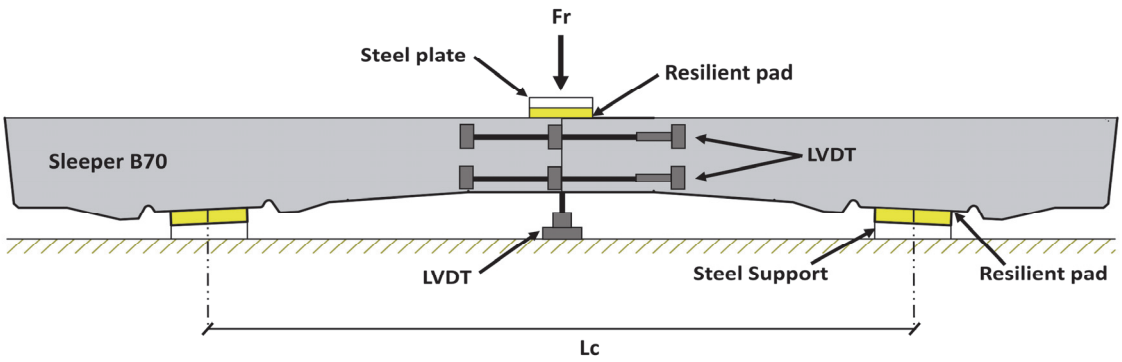

(b)

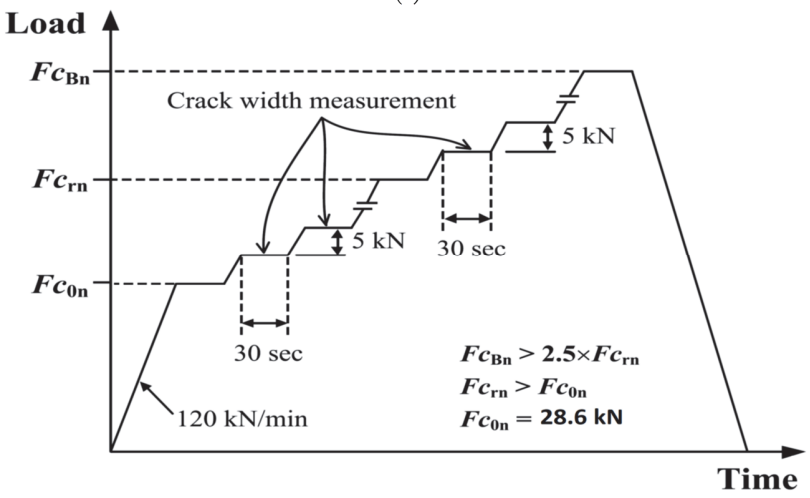

(c)

Figure 8: Static bending test at center section: (a) test setup; (b) test setup sketch; (c) loading protocol [30,31].

Pull-out tests of fasting system

The rail fastening system is based on the connection between the screw and the plastic dowel, which bonded to the concrete sleepers. However, it is known that during operation, the collapse of the plastic dowel and the uplift of the screw is observed. Therefore, the pull-out test was carried out following EN 13481-2 [19]. The uplift load protocol applied as follows: (1) the screw was loaded upwards by a vertical force using a hydraulic jack until the force reached 60 kN; (2) the load was preserved for three minutes, and the sleeper was checked for cracks; (3) The load was increased until reach the stage of collapse or pull-out of the screw. knowing that the lifting loading rate was 50 ± 10 kN/min. The test setup is shown in Fig. 9 as a present by EN 13481-2 [19].

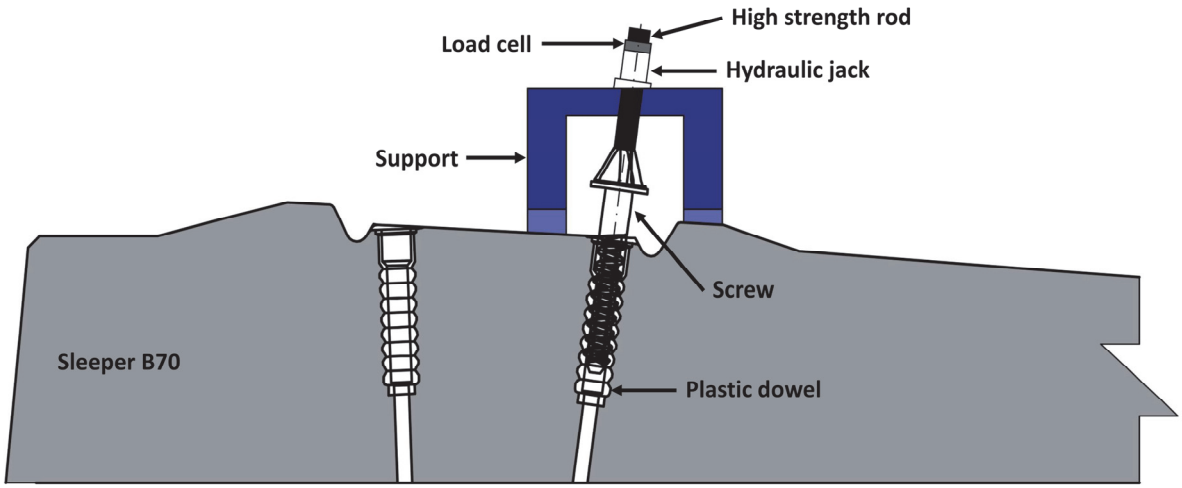

Figure 9: Pull-out test setup.

EXPERIMENTAL RESULTS

Static bending test at rail-seat section

The applied load versus midspan deflection responses for all sleepers (three sleepers for each variable) are shown in Fig. 10. During the bending test, the relationship between applied load and the crack width be recorded and presented in Fig. 11. At the end of the test, the failure modes of the sleepers are clarified in Fig. 12 and 13. However, the failure modes and the test values are also summarized in Tab. 6. Furthermore, the failure modes and the result value were varied, even though all three sleepers were designed to have the same capacity and materials. That's because the complex stress distribution in the short spans made resulted in different failure modes [30].

The three specimens of normal concrete sleepers (SN series) exhibited the first crack at the range from 242.4 kN to 258.3 kN and resulted in failure loads ranging from 362.7 kN to 374.6 kN. At the peak load, specimen no.1 exhibited a sudden drop in load because of the compression failure at the top of the sleeper and the shear failure under the loading plate at a deflection of 15.87 mm, as shown in Fig. 10(a) and 12(a). However, specimen no.2 had a higher failure load compared with the other specimens for the same series until a deflection of 18.2 mm, followed by a drop in the load due to the failure at the edge of the sleeper as shown in Fig. 10(a) and 12(b). In addition, Specimen no.3 had the lower load compared with the other two specimens until a deflection of 15.5 mm and exhibited a sudden drop in the load with the formation of a flexural-shear crack.

On the other hand, the three specimens of UHPC sleepers (S0 series) exhibited the first crack at the range from 255.7 kN to 287.9 kN and resulted in failure loads ranging from 420.15 kN to 424.32 kN. The collapse shape of the first sample in this group was the same as the collapse of the first sample in the previous group, as shown in Fig. 13(a), but it had a maximum failure load of 424.3 kN at a deflection of about 19.8 mm as shown in Fig. 10(b). However, specimens no.2 exhibited a sudden drop in load because of a flexural-shear failure at a deflection of 12.1 mm, as shown in Fig. 10(b) and 13(b). Specimens no.3 had the same failure shape as Specimens no.1 with a maximum deflection at the group 22.7 mm, as shown in Fig. 10(b) and 13(c).

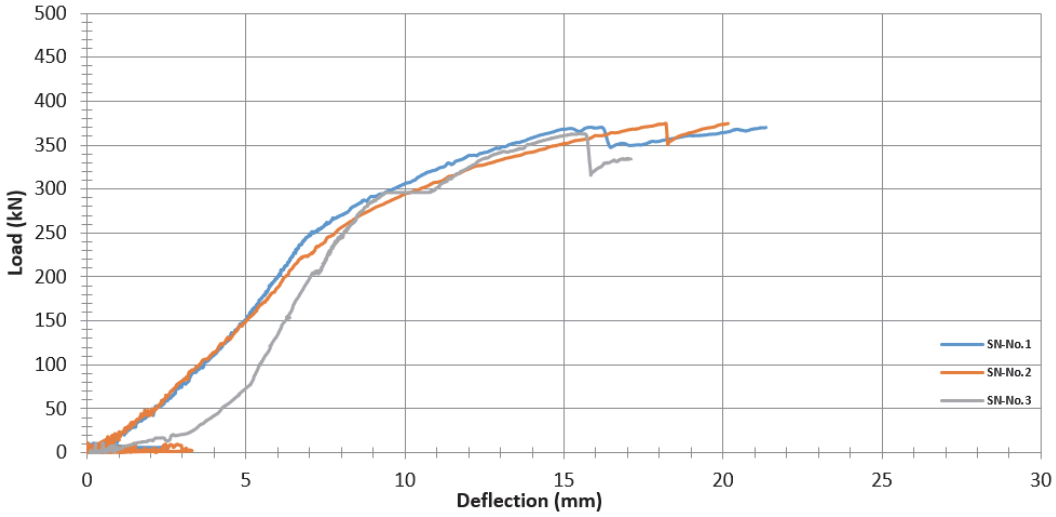

(a)

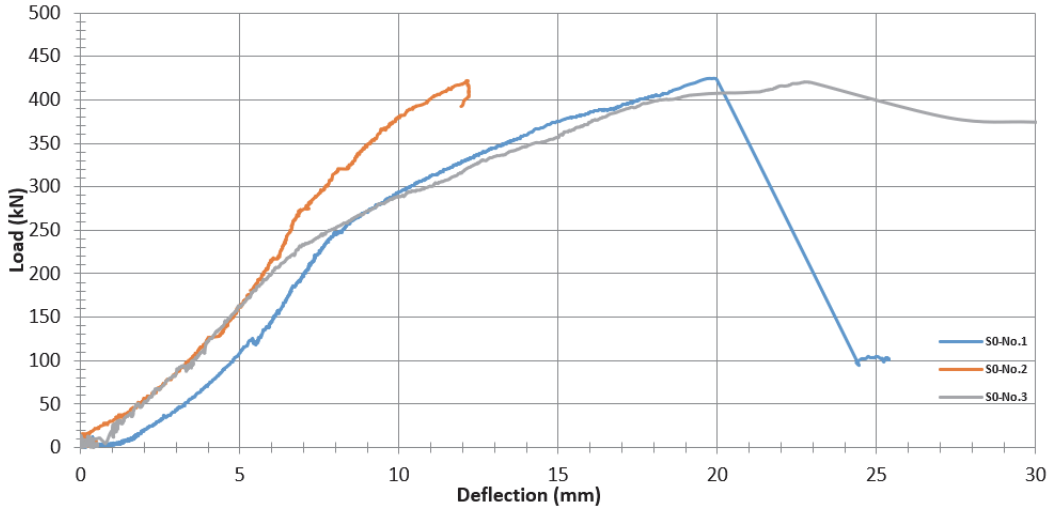

(b)

Figure 10: Load versus deflection responses for static bending test at rail seat section: (a) SN; (b) S0.

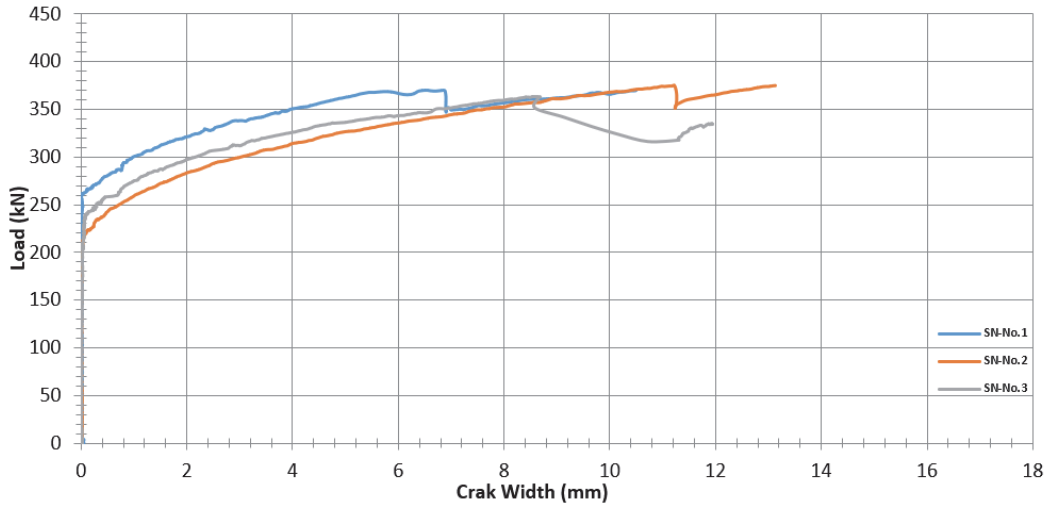

(a)

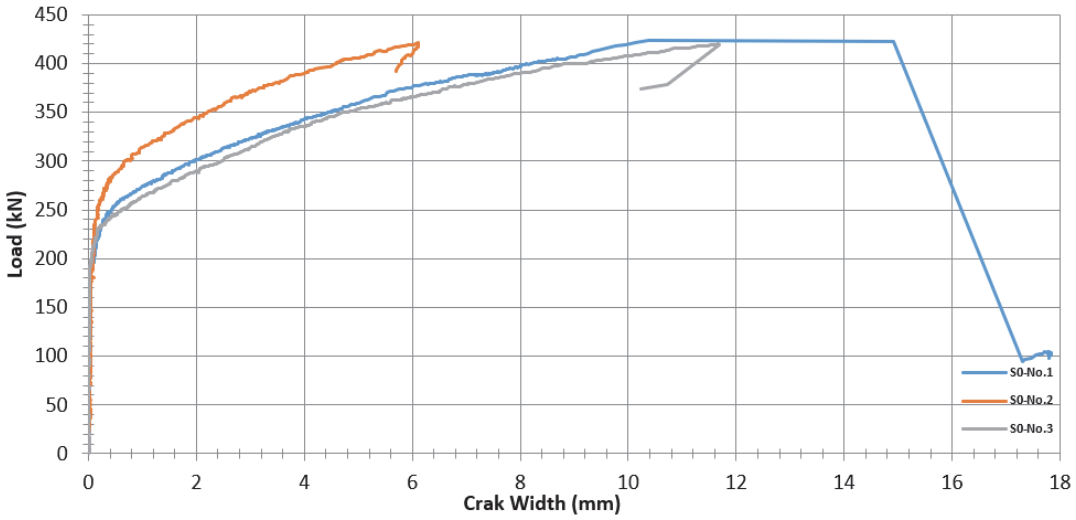

(b)

Figure 11: Load versus crack width responses for static bending test at rail seat section: (a) SN; (b) S0.

(a)

(b)

(c)

Figure 12: Typical failure modes of normal concrete sleepers at rail seat section: (a) SN-No.1; (b) SN-No.2; (c) SN-No.3.

(a)

(b)

(c)

Figure 13: Typical failure modes of UHPC concrete sleepers at rail seat section: (a) S0-No.1; (b) S0-No.2; (c) S0-No.3.

Sleeper series	Number	First cracking	Failure load	Failure mode
		$Fr_r > 130$ kN	$Fr_B > 325$ kN	
SN	No.1	251.5 kN	370.06 kN	Shear and compression failure
	No.2	242.4 kN	374.62 kN	Failure at the edge
	No.3	258.3 kN	362.71 kN	Flexural-Shear failure
	Avg.	250.73 kN	369.13 kN	
S0	No.1	264.5 kN	424.32 kN	Shear and compression failure
	No.2	287.9 kN	421.15 kN	Flexural-shear failure
	No.3	255.7 kN	420.15 kN	Shear and compression failure
	Avg.	269.4 kN	422.05 kN	

Table 6: Results of static bending test at rail seat section.

Static bending test at center section

The applied load versus midspan deflection responses of a set of two sleepers for each variable are shown in Fig. 14. During the test, the thickness of the cracks resulting from the loading is recorded in Fig. 15. The failure modes of the specimens are clarified for each variable in Fig. 16 and 17. The test result and the failure modes are summarized in Tab. 7.

The normal concrete sleepers (SN series) revealed the first crack at an average load of 51 kN, and the failure loads average 91.6 kN at the static bending test at the center section. The failure mode shape for specimen no.4 was the flexural-shear cracking with concrete crushing at the top of the center section at failure load 89.1 kN with a maximum deflection at midspan of the sleeper was 40 mm as shown in Fig. 14(a) and 16(a). However, specimen no.4 had a failure load of 94.1 kN with a maximum deflection at midspan 35.8 mm, as shown in Fig. 14(a). In addition, the failure mode shape for specimen no.5 was the flexural-shear cracking with bond splitting along the strand and with concrete crushing at the end edge of the sleeper around the wires, as shown in Fig. 16(b).

On the other hand, the two specimens of UHPC sleepers (S0 series) exhibited the first crack at the average 63 kN and resulted in failure loads in an average of 106.7 kN. The failure mode shape of the first sample in this group was the same as the collapse of the second sample in the previous group, as shown in Fig. 17(a), but it had a maximum failure load of 109.2 kN at a deflection of about 39.5 mm as shown in Fig. 14(b). However, the failure mode shape for specimens no.5 was flexural-shear cracking in addition to the wire exit out from its position at maximum load 104.2 kN with deflection of 45 mm, as shown in Fig. 14(b) and 17(b).

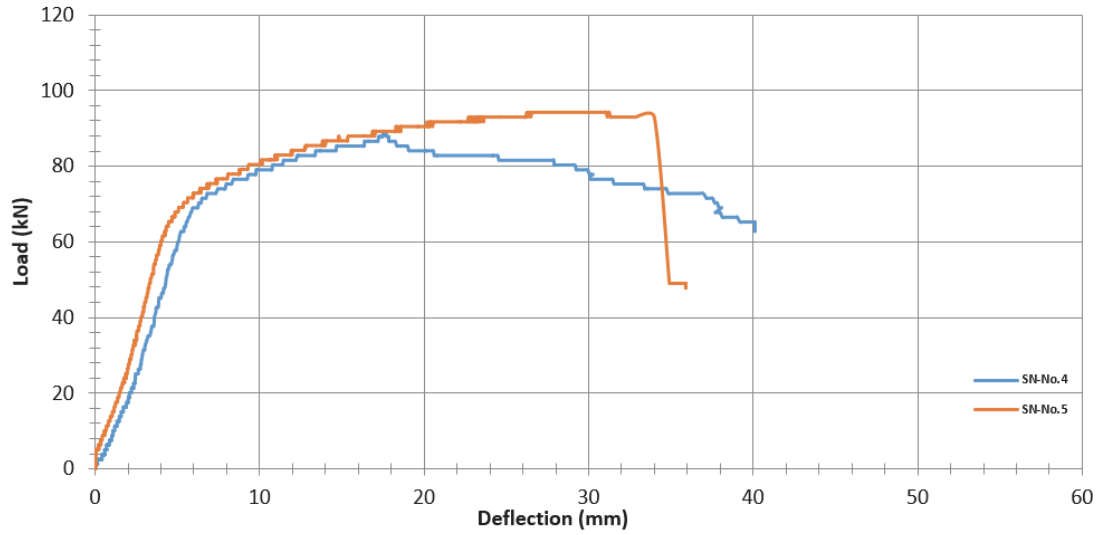

(a)

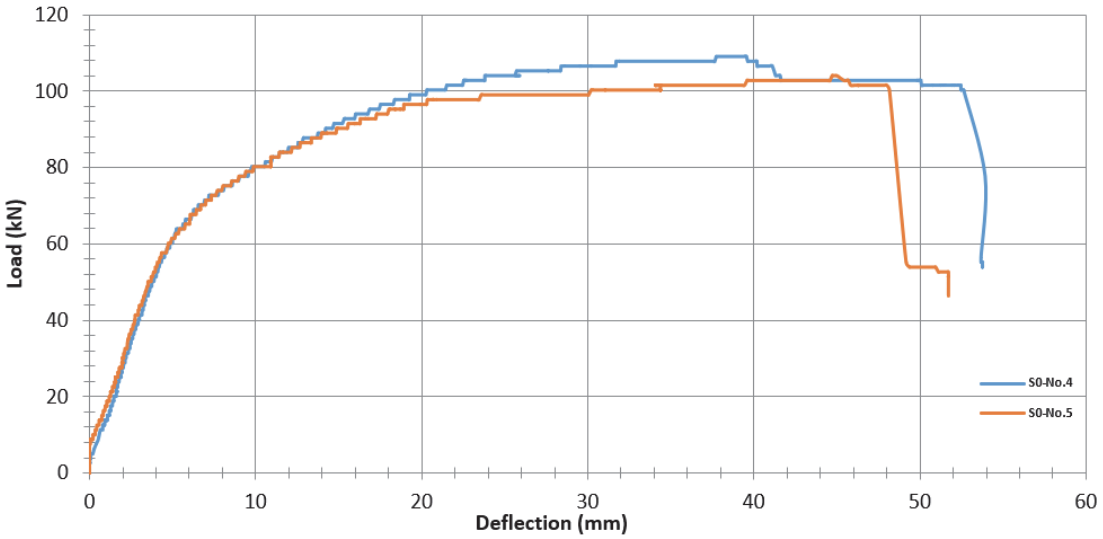

(b)

Figure 14: Load versus deflection responses for static bending test at center section: (a) SN; (b) S0.

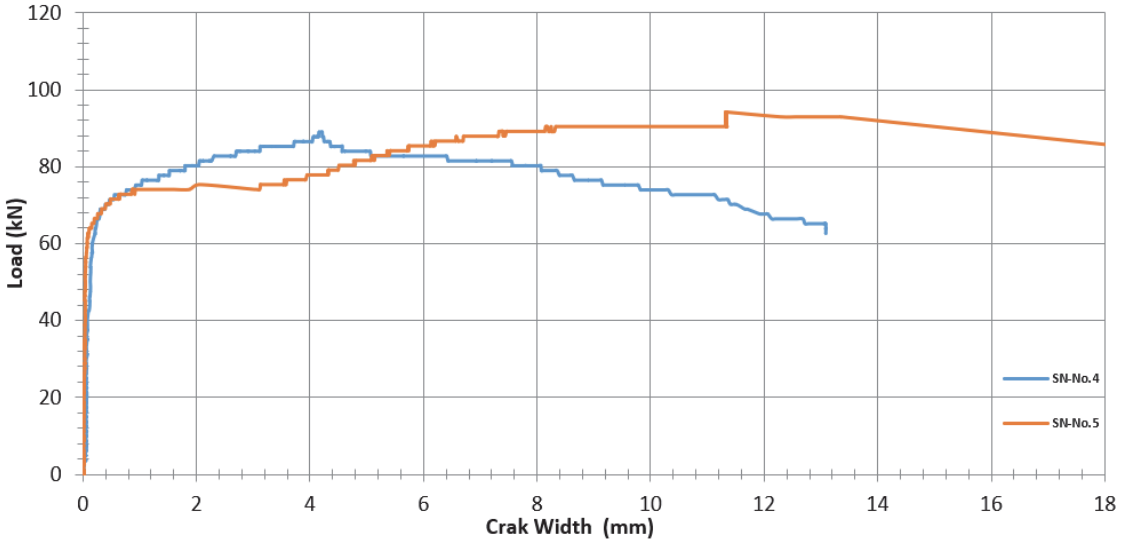

(a)

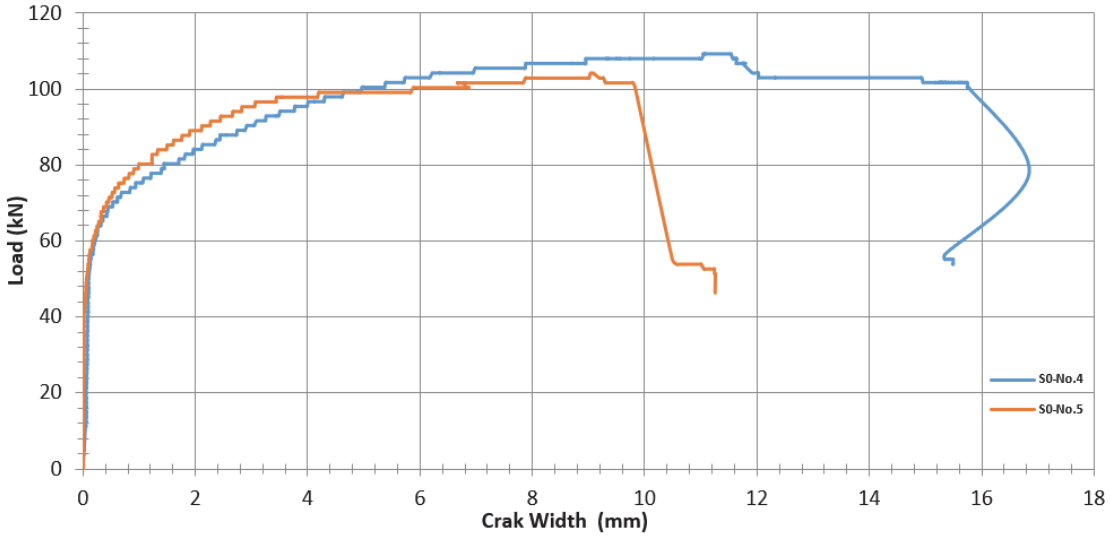

(b)

Figure 15: Load versus crack width responses for static bending test at center section: (a) SN; (b) S0.

(a)

(b)

Figure 16: Typical failure modes of normal concrete sleepers at rail seat section: (a) SN-No.4; (b) SN-No.5.

(a)

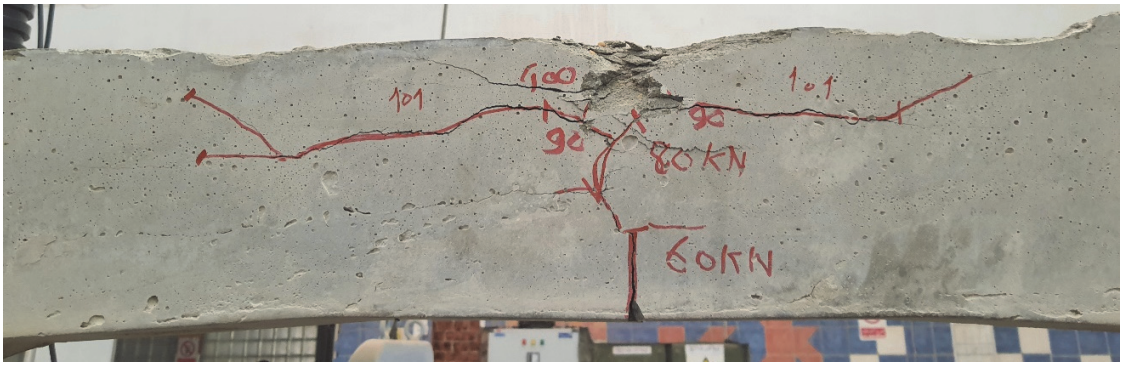

(b)

Figure 17: Typical failure modes of UHPC concrete sleepers at rail seat section: (a) S0-No.4; (b) S0-No.5.

Sleeper series	Number	First cracking	Failure load	Failure mode
		Fc_n > 30 kN	Fc_B > 75 kN	
SN	No.4	52 kN	89.1 kN	Flexural-shear cracking with concrete crushing
	No.5	50 kN	94.12 kN	Flexural-shear cracking with bond splitting along the strand
	Avg.	51 kN	91.61 kN	
S0	No.4	66 kN	109.18 kN	Flexural-shear cracking with bond splitting along the strand
	No.5	60 kN	104.16 kN	Flexural-shear cracking with concrete crushing
	Avg.	63 kN	106.67 kN	

Table 7: Results of static bending test at rail seat section.

Pull-out tests of fasting system

The pull-out test results for the rail fasting system summarizes in Tab. 7. During the test, the tension load versus screws exit distance for two sleepers for each variable are shown in Fig. 18. Fig. 19 shows the failure shape of the sleepers after the pull-out tests. All the sleepers had no cracks at load 60 kN of the pull-out tests and were maintained for three minutes. For normal concrete sleepers, the tensile failure happened at an average load of 112.6 kN with a maximum average displacement for the screw was 18 mm, as shown in Fig. 18(a). On the other hand, for UHPC sleepers, the tensile failure happened at an

average load of 107.6 kN with a maximum average displacement for the screw was 31.2 mm, as shown in Fig. 18(b). In addition, the failure shape for normal concrete was confined to the existence of the plastic dowel from its position, as shown in Fig. 19. However, the failure shape for UHPC sleepers was a fracture in the concrete, as shown in Fig. 20.

Sleeper series	Number	Crack inspection at a load of 60 kN	Fracture load
SN	No.6	No cracks	109 kN
	No.7	No cracks	116.3 kN
	Avg.		112.6 kN
S0	No.6	No cracks	106.6 kN
	No.7	No cracks	108.7 kN
	Avg.		107.6 kN

Table 8: Pull-out test result.

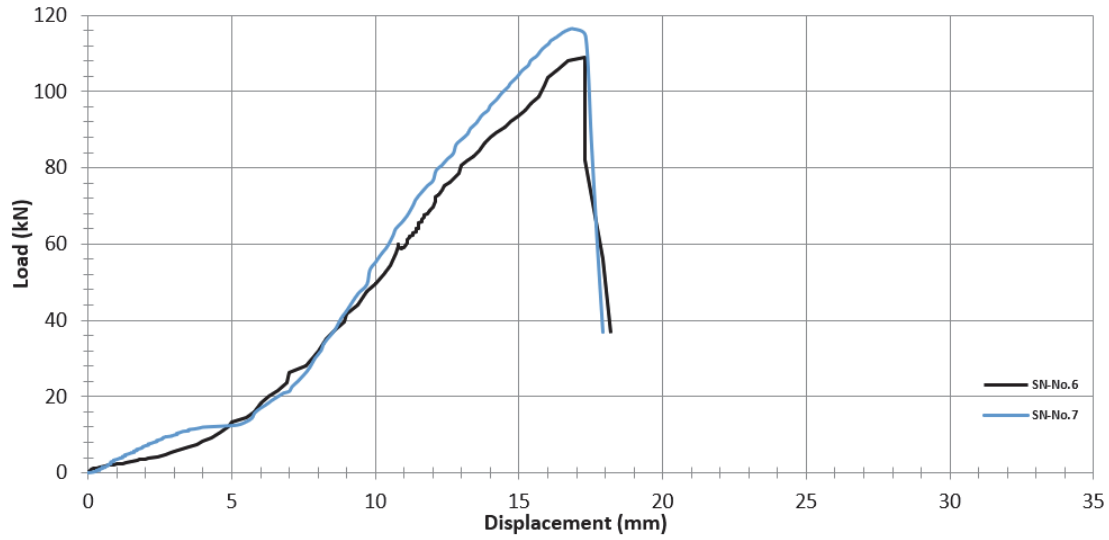

(a)

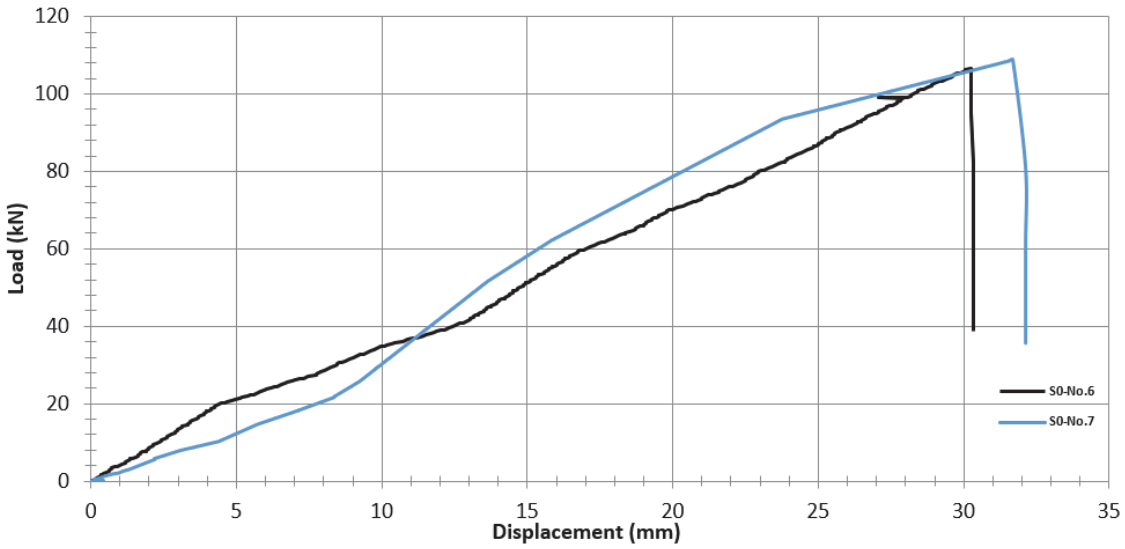

(b)

Figure 18: Load versus screws exit distance pull-out test: (a) SN; (b) S0.

(a)

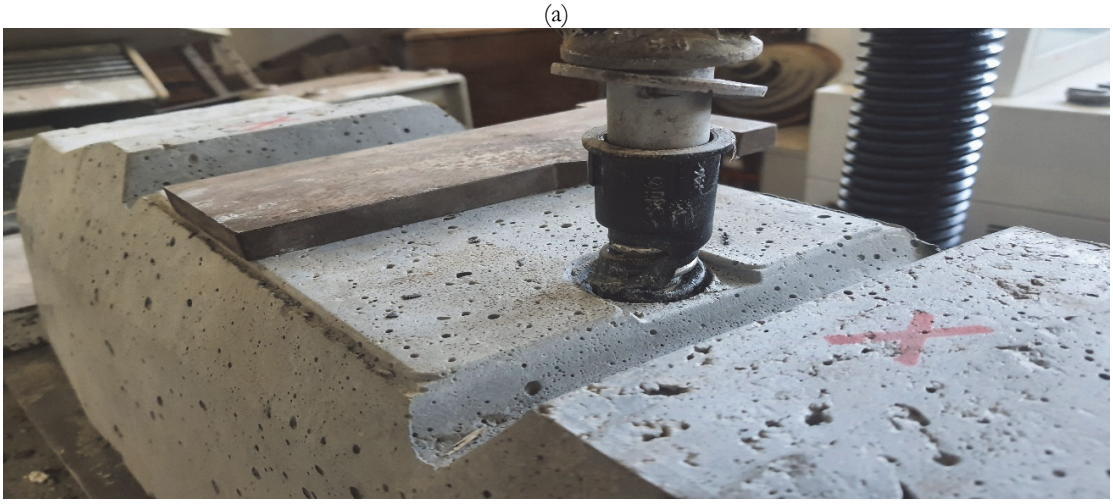

(b)

Figure 19: The failure shape of the sleepers after the pull-out test: (a) SN-No.6; (b) SN-No.7.

(a)

(b)

Figure 20: The failure shape of the sleepers after the pull-out test: (a) S0-No.6; (b) S0-No.7.

Conclusion

In this investigation, a UHPC sleeper B70 was developed and fabricated for the first time to study the extent of the change resulting from this mixture. A series of structural tests included a static bending test at the rail seat section and center section, and the pull-out test were conducted following EN 13230-2 and EN 13481-2 [18,19]. Based on the results of experimental work, the following point can be concluded:

(1) To explore the effect of employing UHPC in concrete sleepers, we employed fine material to improve workability and generate a UHPC mixture used for casting sleepers (B70) with a compressive strength of 102 MPa after 28 days of curing (B70).
(2) The average first cracking load of UHPC sleepers for the static bending test at the rail seat section and the center section were 2 times and 2.1 times higher than the reference value, respectively. In addition, the average failure load for the same tests were 1.3 times and 1.4 times higher than the reference values, respectively.
(3) The result of the static bending test at the rail seat section and the center section showed that the failure load for UHPC sleepers was higher than the conventional concrete sleeper.
(4) The pull-out resistance for the screws at UHPC sleepers exceeded the minimum requirement of EN 13481-2 [19].
(5) The average pull-out load of UHPC sleepers was approximately equal for the conventional concrete.

It is expected that this experimental research will provide some information about the UHPC that can be used in the railway field. As an extension of the present study, using steel fiber in the UHPC mixture is currently being conducted to improve the properties and show the effects on the mixture. Additional researches should be conducted in this field to take full advantage of this product in the railway field.

Acknowledgments

All thanks to the National Authority for Tunnels for the facilities to produce our specimens from Siegwart factory. The authors are thankful for the teamwork of the Housing and Building National Research Center, Egypt.

References

[1] Kaewunruen, S., Remennikov, A.M. (2009). Progressive failure of prestressed concrete sleepers under multiple high-intensity impact loads, Eng. Struct., 31(10), pp. 2460–2473, DOI: 10.1016/j.engstruct.2009.06.002.

[2] Kaewunruen, S., Remennikov, A.M. (2010). Dynamic Crack Propagations in Prestressed Concrete Sleepers in Railway Track Systems Subjected to Severe Impact Loads, J. Struct. Eng., 136(6), pp. 749–754, DOI: 10.1061/(asce)st.1943-541x.0000152.
[3] Manalo, A., Aravinthan, T., Karunasena, W., Ticoalu, A. (2010). A review of alternative materials for replacing existing timber sleepers, Compos. Struct., pp. 603–611, DOI: 10.1016/j.compstruct.2009.08.046.
[4] Rothlisberger, E. History and development of wooden sleeper. Available at: https://www.groupe-corbat.ch/files/4/Timber_sleeper-history_and_development.pdf.
[5] Berbey Alvarez, A., Guevara-Cedeño, J. (2020).Railway Engineering., Oxford University Press, pp. 371–395.
[6] Shan, L. (2012).Railway Sleeper Modelling with Deterministic and Non-deterministic Support Conditions Master Degree Project.
[7] Sadeghi, J., Barati, P. (2012). Comparisons of the mechanical properties of timber, steel and concrete sleepers, Struct. Infrastruct. Eng., 8(12), pp. 1151–1159, DOI: 10.1080/15732479.2010.507706.
[8] Bae, Y., Pyo, S. (2020). Effect of steel fiber content on structural and electrical properties of ultra high performance concrete (UHPC) sleepers, Eng. Struct., 222, DOI: 10.1016/j.engstruct.2020.111131.
[9] Lutch, R.H. (2009). Capacity Optimization of a Prestressed Concrete Railroad Tie, , pp. 230, DOI: 10.37099/mtu.dc.etds/254.
[10] Sadeghi, J.M., Babaee, A. (2006). Structural optimization of B70 railway prestressed concrete sleepers, 30.
[11] ACI 239R-18. (2018). Ultra-high-performance concrete: An emerging technology report, MI, USA, American Concrete Institute (ACI).
[12] Hussein, L., Amleh, L. (2015). Structural behavior of ultra-high performance fiber reinforced concrete-normal strength concrete or high strength concrete composite members, Constr. Build. Mater., 93, pp. 1105–1116, DOI: 10.1016/j.conbuildmat.2015.05.030.
[13] Safdar, M., Matsumoto, T., Kakuma, K. (2016). Flexural behavior of reinforced concrete beams repaired with ultra-high performance fiber reinforced concrete (UHPFRC), Compos. Struct., 157, pp. 448–460, DOI: 10.1016/j.compstruct.2016.09.010.
[14] Hajar, Z., Resplendino, J., Lecointre, D., Petitjean, J., Simon, A. (2004).Ultra-high-performance concretes: First recommendations and examples of application. Proceedings of the fib Symposium 2004 - Concrete Structures: The Challenge of Creativity, pp. 242–243.
[15] Yu, R., Spiesz, P., Brouwers, H.J.H. (2015). Development of an eco-friendly Ultra-High Performance Concrete (UHPC) with efficient cement and mineral admixtures uses, Cem. Concr. Compos., 55, pp. 383–394, DOI: 10.1016/j.cemconcomp.2014.09.024.
[16] Tayeh, B.A., Abu Bakar, B.H., Megat Johari, M.A., Voo, Y.L. (2012). Mechanical and permeability properties of the interface between normal concrete substrate and ultra high performance fiber concrete overlay, Constr. Build. Mater., 36, pp. 538–548, DOI: 10.1016/j.conbuildmat.2012.06.013.
[17] Hassan, A. (2013). Ultra high performance fibre reinforced concrete for highway bridge applications, (June), pp. 24.
[18] EN 13230-2. (2009). Railway applications - Track - Concrete sleepers and bearers - Part 2: Prestressed mono-block sleepers, Brussles, Belgium, European Committee for Standardization (CEN).
[19] EN 13481-2. (2014). Railway applications - Track - Performance requirements for fastening systems - Part 2: Fastening systems for concrete sleepers, Brussles, Belgium, European Committee for Standardization (CEN).
[20] EN 10138-2. (2000). Prestressing steels - Part 2: Wire Armatures, Brussles, Belgium, European Committee for Standardization (CEN).
[21] Yu, R., Spiesz, P., Brouwers, H.J.H. (2014). Mix design and properties assessment of Ultra-High Performance Fibre Reinforced Concrete (UHPFRC), Cem. Concr. Res., 56, pp. 29–39, DOI: 10.1016/j.cemconres.2013.11.002.
[22] EN 13230-1. (2016). Railway applications - Track - Concrete sleepers and bearers - Part 1: General requirements, Brussles, Belgium, European Committee for Standardization (CEN).
[23] Mo, Z., Gao, X., Su, A. (2021). Mechanical performances and microstructures of metakaolin contained UHPC matrix under steam curing conditions, Constr. Build. Mater., 268, DOI: 10.1016/j.conbuildmat.2020.121112.
[24] Qian, D., Yu, R., Shui, Z., Sun, Y., Jiang, C., Zhou, F., Ding, M., Tong, X., He, Y. (2020). A novel development of green ultra-high performance concrete (UHPC) based on appropriate application of recycled cementitious material, J. Clean. Prod., 261, pp. 121231, DOI: 10.1016/j.jclepro.2020.121231.
[25] Alani, A.H., Bunnori, N.M., Noaman, A.T., Majid, T.A. (2019). Durability performance of a novel ultra-high-performance PET green concrete (UHPPGC), Constr. Build. Mater., 209, pp. 395–405, DOI: 10.1016/j.conbuildmat.2019.03.088.
[26] Gautham Kishore Reddy, G., Ramadoss, P. (2020). Influence of alccofine incorporation on the mechanical behavior of

ultrahigh performance concrete (UHPC), Mater. Today Proc., 33(xxxx), pp. 789–797, DOI: 10.1016/j.matpr.2020.06.180.

[27] Yu, R., Spiesz, P., Brouwers, H.J.H. (2015). Development of Ultra-High Performance Fibre Reinforced Concrete (UHPFRC): Towards an efficient utilization of binders and fibres, Constr. Build. Mater., 79, pp. 273–282, DOI: 10.1016/j.conbuildmat.2015.01.050.

[28] UIC. 713R. (2004).Design of Monoblock Concrete Sleepers., International Union of Railways, p. 30.

[29] EN 13230-6. (2014). Railway applications - Track - Concrete sleepers and bearers - Part 6: Design, Brussles, Belgium, European Committee for Standardization (CEN).

[30] Yang, J.M., Shin, H.O., Yoon, Y.S., Mitchell, D. (2017). Benefits of blast furnace slag and steel fibers on the static and fatigue performance of prestressed concrete sleepers, Eng. Struct., 134, pp. 317–333, DOI: 10.1016/j.engstruct.2016.12.045.

[31] Yoo, D.Y., Lee, J.Y., Shin, H.O., Yang, J.M., Yoon, Y.S. (2019). Effects of blast furnace slag and steel fiber on the impact resistance of railway prestressed concrete sleepers, Cem. Concr. Compos., 99, pp. 151–164, DOI: 10.1016/j.cemconcomp.2019.03.015.